International Journal of Mass Spectrometry 283 (2009) 200–205

Contents lists available at ScienceDirect

International Journal of Mass Spectrometry

journal homepage: www.elsevier.com/locate/ijms

Internal energy deposition with silicon nanoparticle-assisted laser desorption/ionization (SPALDI) mass spectrometry

Shai Dagan[1], Yimin Hua, Dylan J. Boday, Arpad Somogyi, Ronald J. Wysocki, Vicki H. Wysocki*

Department of Chemistry, University of Arizona, 1306 E University Boulevard, Tucson, AZ 85721, USA

ARTICLE INFO

Article history:
Received 16 January 2009
Received in revised form 14 March 2009
Accepted 19 March 2009
Available online 9 April 2009

Keywords:
Silicon nanoparticles
Laser desorption/ionization
Matrix-less
Matrix-free
Soft ionization

ABSTRACT

The use of silicon nanoparticles for laser desorption/ionization (LDI) is a new appealing matrix-less approach for the selective and sensitive mass spectrometry of small molecules in MALDI instruments. Chemically modified silicon nanoparticles (30 nm) were previously found to require very low laser fluence in order to induce efficient LDI, which raised the question of internal energy deposition processes in that system. Here we report a comparative study of internal energy deposition from silicon nanoparticles to previously explored benzylpyridinium (BP) model compounds during LDI experiments. The internal energy deposition in silicon nanoparticle-assisted laser desorption/ionization (SPALDI) with different fluorinated linear chain modifiers (decyl, hexyl and propyl) was compared to LDI from untreated silicon nanoparticles and from the organic matrix, α-cyano-4-hydroxycinnamic acid (CHCA). The energy deposition to internal vibrational modes was evaluated by molecular ion survival curves and indicated that the ions produced by SPALDI have an internal energy threshold of 2.8–3.7 eV. This is slightly lower than the internal energy induced using the organic CHCA matrix, with similar molecular survival curves as previously reported for LDI off silicon nanowires. However, the internal energy associated with desorption/ionization from the silicon nanoparticles is significantly lower than that reported for desorption/ionization on silicon (DIOS). The measured survival yields in SPALDI gradually decrease with increasing laser fluence, contrary to reported results for silicon nanowires. The effect of modification of the silicon particle surface with semifluorinated linear chain silanes, including fluorinated decyl (C10), fluorinated hexyl (C6) and fluorinated propyl (C3) was explored too. The internal energy deposited increased with a decrease in the length of the modifier alkyl chain. Unmodified silicon particles exhibited the highest analyte internal energy deposition. These findings may suggest a role of the modifier as a moderator in the energy dissipation and relaxation process. The relatively low internal energy content of SPALDI-produced ions indicates that this is a “soft” desorption technique, with potential advantages in the analysis of labile compounds.

1. Introduction

Matrix-assisted laser desorption/ionization (MALDI), first introduced in the late 1980s [1], has become a popular technique for mass spectral analysis of large molecules. The application of MALDI has also extended to fast screening, and recently also to imaging of small molecules, especially polar, ionic and/or thermally labile compounds. In order to allow the analysis of small molecules (typically < 500 Da) on MALDI instruments, several approaches have been explored to overcome the low-mass chemical background associated with the organic ionizing matrix. Among them, matrix-less approaches have received considerable attention in the last decade. Silicon, which absorbs UV efficiently, was found to be a successful substrate for matrix-less laser desorption/ionization (LDI). A new technique, desorption/ionization on silicon (DIOS), which was invented [2], extensively explored [3–5] and improved by Siuzdak and co-workers [6], became a commercially viable option, with attractive applications mainly for basic compounds such as drugs and metabolites. Other approaches using silicon in LDI experiments involved the use of particles, first in the micro-scale [7] and later in the nanoscale. Two-dimensional nanostructures of silicon, such as silicon nanotubes [8,9] and silicon nanowires (10–40 nm diameter) grown on silicon surfaces [10], have shown to induce efficient LDI. Silicon nanoparticles were first introduced as a promising matrix-less substrate for LDI by Credo and Bouvier [11]. Recently, this approach, now referred to as silicon nanoparticle-assisted laser desorption/ionization (SPALDI), was further developed, explored and improved, to become a sensitive, selective, robust and low-

---

* Corresponding author.
E-mail address: vwysocki@email.arizona.edu (V.H. Wysocki).

[1] Permanent address: Israel Institute for Biological Research (IIBR), P.O.B. 19, Ness Ziona 74100, Israel.

1387-3806/$ – see front matter © 2009 Elsevier B.V. All rights reserved.
doi:10.1016/j.ijms.2009.03.013

cost technique [12]. Comparing common MALDI as well as DIOS approaches to silicon nanowires and particles, it was observed that lower laser fluences were required for the nanowire and particle approaches [12,13]. This leads to the question of the energy transfer mechanism and the internal energy content of the desorbed ions.

During LDI processes, energy deposition is one of the main factors affecting the dissociation of molecular ions and the resulting mass spectral appearance. Better understanding of those processes may contribute to the development of "softer" ionization methods based on MALDI and LDI approaches. Energy transfer processes and internal energy of ions produced in LDI assisted by various matrices as well as under different operating conditions, have been investigated by Zenobi and co-workers [14–16], Karas and co-workers [17,18] and Vertes and co-workers [13,19–21]. Using substituted benzylpyridinium (BP) preionized salts as model compounds, Vertes and co-workers demonstrated the difference in energy transfer among several conventional chemical matrices by comparing the survival yields of the molecular ions [19] and explored the effects of laser pulse duration on the internal energy content of the ions [20]. The Vertes group also investigated energy transfer during LDI from DIOS chips [21] and recently from silicon nanowires [13]. It appears that DIOS induces more internal energy than standard chemical matrices such as α-cyano-4-hydroxycinnamic acid (CHCA). LDI on nanowire structures, on the other hand, is much softer and the internal energy deposited is reported to be comparable to CHCA.

Here we report on comparative measurements for the internal energy deposition during LDI using silicon nanoparticles. The data presented here provide additional knowledge on the heat transfer processes on silicon, which may improve the understanding of the role of the morphological structure (flat surfaces vs. nanostructures) as well as the function of chemical modifications on LDI. Following Vertes and co-workers [13,19–22] the BP model compounds were used and their molecular ion survival yields served to estimate the internal energy of the desorbed ions from modified and unmodified silicon nanoparticles. For comparison, energy deposition from CHCA was measured as well.

2. Experimental

2.1. Preparation of Si powder

The LDI-optimized preparation procedure of the silicon was presented and discussed in detail previously [12]. Briefly, 8 mg of 30 nm silicon nanoparticles (Meliorum Technologies Inc., Rochester, NY, USA) were treated by 0.4 mL 10% HNO_3 directly for 30 min with sonication in a heated water bath at ∼45 °C. The powder was then centrifuged, followed by two cycles of washing by isopropanol and centrifugation thereafter to remove the HNO_3. Finally, the powder was dried in a vacuum concentrator (SpeedVac®Plus SC110A, Thermo Savant, Holbrook, NY, USA), heated to 40 °C for 2 h. The dried powder was silylated with 90 μL neat (heptadecafluoro-1,1,2,2-tetrahydrodecyl)dimethylchlorosilane (C10) (Gelest Inc., Morrisville, PA, USA) for 30 min under sonication, and then dried in an oven at 90 °C for about 24 h (note that we have also recently optimized a solution preparation). Comparative experiments were performed by modifying the silicon nanopowder with nonafluorohexyltrichlorosilane (C6) and (3,3,3-trifluoropropyl)trichlorosilane (C3), also from Gelest Inc. (Morrisville, PA, USA), using the same procedure as described above.

Finally, the silylated silicon nanoparticles were stored in 0.4 mL perfluorohexane for later use after drying of the powder. Before application of the powder on a MALDI plate, the perfluorohexane was replaced with isopropanol. A suspension of powder in fresh isopropanol was achieved by sonication, followed by the addition and mixing of Milli-Q water to obtain a final ratio of isopropanol to water of 2:1 (v/v). Untreated silicon nanoparticles were only washed with isopropanol and finally dispersed in isopropanol:water (2:1, v/v) before application.

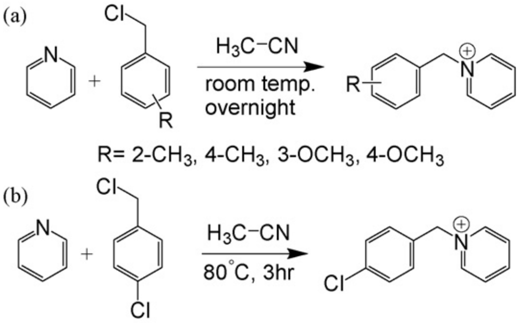

Scheme 1. Preparation of the benzylpyridium salts.

2.2. Materials and analyte sample preparation

Five benzylpyridinium (BP) salt derivatives were prepared: 2-methyl, 4-methyl, 3-methoxy, 4-methoxy and 4-chloro BP's as illustrated in Scheme 1. Except for 4-chloro BP, the benzylpyridinium salts were prepared by reaction of the appropriately substituted benzylic chloride (Acros Organics, Geel, Belgium) with 1.2 equivalents of pyridine in dry acetonitrile solvent stirred with a magnetic stir bar overnight at room temperature as shown in Scheme 1(a). Scheme 1(b) describes that the reaction of pyridine with *p*-chlorobenzyl chloride required warming the reaction mixture at reflux for 3 h to make 4-chloro BP. Diethyl ether was added to the reaction solution to precipitate out the benzyl pyridinium salts. The solids were collected by filtration and washed with anhydrous hexanes. These salts were very hygroscopic and require storage in a vacuum desiccator over anhydrous calcium sulfate. The yields for these reactions were between 73 and 84%.

Stock solutions of the BP salts (typically 1 mg/mL) were prepared in Milli-Q water. Potential organic impurities in the solutions were roughly extracted by dichloromethane. Then the stock solutions of the BP salts were further diluted in Milli-Q water to obtain a final concentration of 20 pmol/μL.

For SPALDI experiments, 1 μL of silicon nanoparticle suspension was spotted on a standard MALDI plate. Before the nanoparticle suspension was allowed to dry, 1 μL of the 20 pmol/μL BP solution was added. To conduct comparative measurements with the CHCA matrix, sample solutions were prepared by mixing saturated CHCA solution and 40 pmol/μL BP solution at a 1:1 (v/v) ratio to achieve a final BP concentration of 20 pmol/μL. The spotted MALDI plate was air dried before introducing it in the MALDI-MS.

2.3. Mass spectrometry

All the experiments were carried out using a Reflex III (Bruker, Billerica, MA, USA) time-of-flight mass spectrometer operated in the positive-ion, reflectron mode. The mass spectrometer was equipped with a standard 337 nm nitrogen laser (LSI-Laser Science Inc., Newton, MA). The laser has an average maximal fluence of 400 μJ/pulse with a focused spot size of ∼100–150 μm in diameter on the MALDI plate. Laser fluences from 1% to 60% of the total fluence (attenuations of 99–40%) were applied. The laser fluence, measured by an external sensor (Coherent-Fieldmate), responded linearly under different attenuation levels. Signals of 50–200 shots were accumulated for each spectrum acquired (3 shots/s). Random rastering of the sample spots was applied, moving typically every 5–10 laser shots.

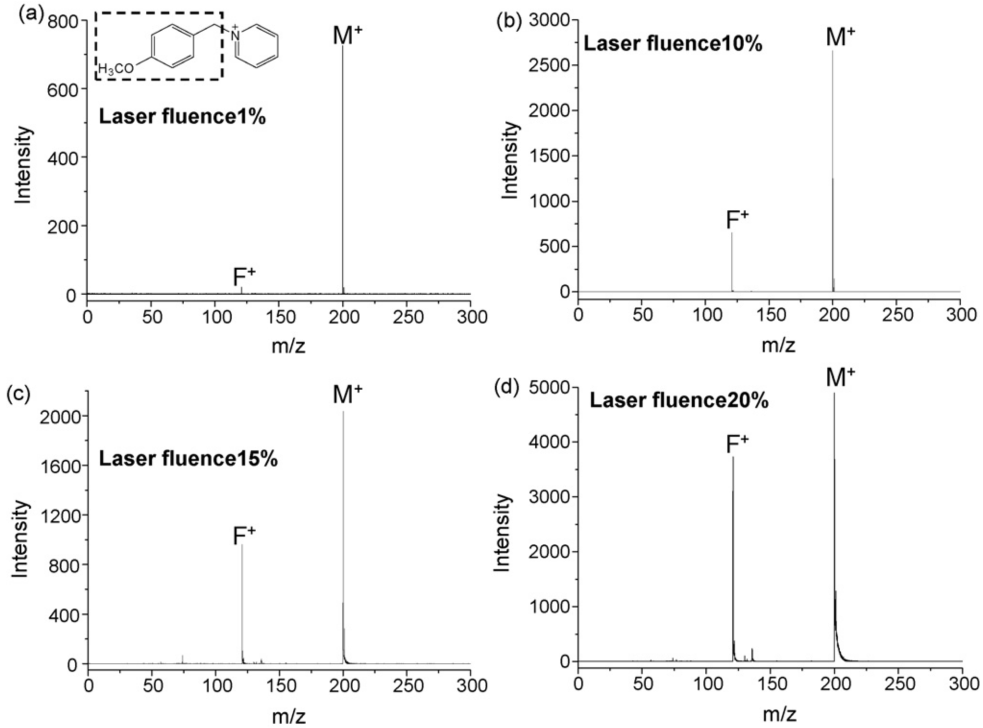

Fig. 1. SPALDI mass spectra of 4-methoxy BP obtained at different laser fluences (1%, 10%, 15%, and 20% of the total fluence). C10 modified particles were used. The major peaks are the molecular ion M$^+$ (*m*/*z* 200) and the methoxybenzyl fragment ion F$^+$ (*m*/*z* 121).

3. Results

The SPALDI spectra of the benzylpyridinium (BP) ions exhibit two primary peaks, the molecular ion and the corresponding fragment (benzyl cation). In Fig. 1, the SPALDI spectra of 4-methoxy BP at four laser fluences (1%, 5%, 10%, 20%) are shown. The relative intensity of the *m*/*z* 121 methoxybenzyl fragment ion increases with the laser fluence consistent with a gradual increase in the ion internal energy. It is noted that the laser fluences used to obtain the high S/N signals shown in Fig. 1 (as low as 1% of the total fluence), are much lower than the fluence threshold required to obtain any signal with common chemical matrices (typically >20% of the total fluence).

The peak tailing present at high laser fluences (Fig. 1(d)) may be due to spatial spread originated by the laser “digging” into the sample spot, while removing some of the nanoparticles. A similar phenomenon was also observed in LDI from silicon nanowires [13].

The molecular ion survival yields of 5 model compounds were measured at different laser fluences, comparing the influence of SPALDI (with chemically modified silicon nanoparticles), LDI on untreated silicon nanoparticles and conventional CHCA chemical matrix on the BP fragmentation. BP molecular survival yields are plotted versus laser fluence in Fig. 2. The laser fluence range presented is from the molecular ion appearance threshold level to the highest level where the signal is still unsaturated. In most cases, fragmentation was observable at the threshold of the molecular ion appearance or slightly above it. The results shown are based on averaged data acquired in several experiments (duplicates or triplicates), with accumulation of 50–200 laser shots per data point per experiment. Typical variance of the reported survival yields is 2–10%.

As shown in Fig. 2, SPALDI exhibits thresholds for ion production at very low laser fluences (1–5% of the maximal fluence). The survival yield of the molecular ions is nearly 100% at the low laser fluences and gradually decreases upon increase of the laser fluence. In the case of SPALDI with C10 derivatized powder, the molecular survival yields are still above 50% even when the laser fluences are raised to 40% of the total fluence. In addition, the total ion signal intensities gradually increase with the laser fluence during SPALDI.

The untreated silicon nanopowder is also an effective substrate for LDI. Compared to SPALDI, the untreated silicon powder LDI provide less analyte sensitivity than the chemically modified particles and exhibits more background peaks, presumably due to surfactants used in the manufacturing process of the silicon nanopowders [12]. The untreated silicon powder has slightly higher laser fluence thresholds for obtaining any signals compared to the chemically modified particles. A possible explanation is that the fluorinated derivatives on the surface of silicon nanoparticles increase the work function of the silicon nanopowder [23] and therefore reduce the neutralization of the precharged BP ions, compared with the untreated silicon nanoparticles, where charge transfer and neutralization is more likely.

The survival yields with the untreated silicon nanoparticles are lower and are usually decreasing upon increase of the laser fluence, similar to SPALDI with silylated powder. The results suggest that the fluorinated modifiers on the silicon nanoparticles play a role in the reduced energy deposition in SPALDI. The inert nature of the fluorinated chain may reduce the energy requirement for analyte evaporation and therefore contribute to the “softer” desorption process. The long chains of the fluorinated derivatives may act as energy moderators that absorb part of the energy which is transferred from the silicon particles to the analytes and thus contribute to more uniform and controllable heat transfer. Similar observations have been reported comparing LDI of tryptophan from octadecyltrichlorosilane-silylated versus unsilylated glass [14], showing less fragmentation in the case of silylated glass.

In order to further explore the influence of the derivatives on the energy deposition in SPALDI, we studied the survival yields of 4-methoxy BP molecules with C6 and C3 modified silicon nanoparticles. These results are included in Fig. 2(c). C6 modification induces survival yields generally lower than C10. The survival yields in the case of C3 derivatization are even lower than

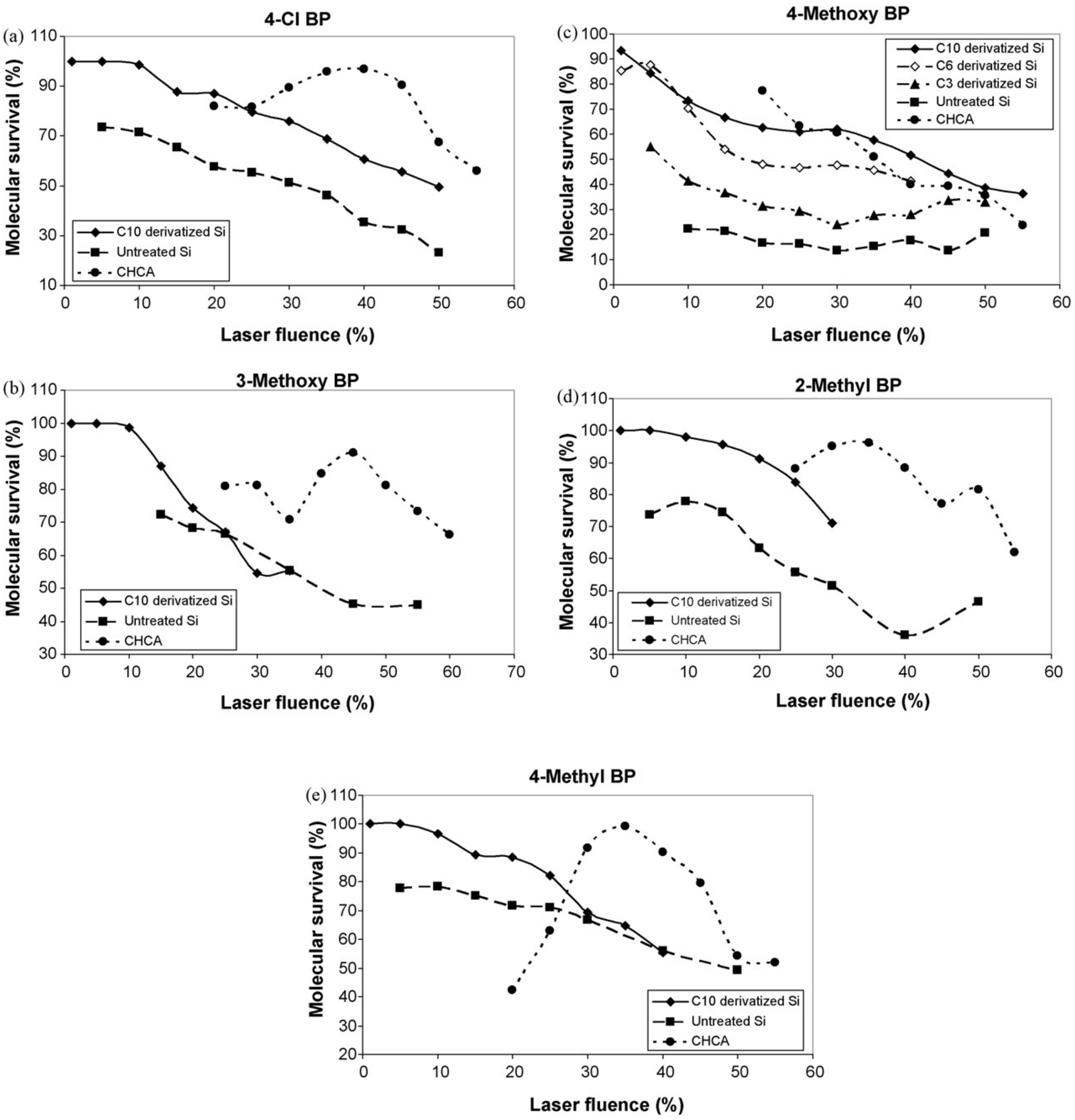

Fig. 2. Molecular ion survival yields (%) for 4-chloro BP (a), 3-methoxy BP (b), 4-methoxy BP (c), 2-methyl BP (d), and 4-methyl BP (e). SPALDI with C10 modified particles (♦), untreated silicon powder (■), CHCA (●), SPALDI with C6 derivatized particles (◇), and SPALDI with C3 derivatized particles (▲). The laser fluence is shown in percentage of the total nitrogen laser fluence. Typical variance of the reported survival yields is 2–10%.

with C6, but still higher than with untreated silicon. The above results further demonstrate that the organic modifiers on the silicon nanoparticle play a role in the energy dissipation and/or relaxation process, depending on the modifier chain length. The laser energy is absorbed efficiently by the silicon particles and then transferred to the analyte on the outer surface through the intermediate layer of the organic modifiers. The rapid surface heating may also involve violent expansion of the fluorinated derivatives with deformation to the surface bulk [24]. The derivatives with longer chains, having more degrees of freedom, are better energy moderators, resulting in "softer" desorption/ionization.

To compare to our results obtained with the modified silicon particles, the BP salts were also analyzed with the previously explored CHCA matrix. Our results indicate that there exists a behavior in which the BP ion survival in MALDI with CHCA is first increasing and then decreasing with the laser fluence. The highest molecular survival yields are obtained when the laser fluences are close to the practical operating level (30–40% of the total laser fluence for CHCA), where intense signals are easy to produce. It is noted that with CHCA the peak intensities at the threshold fluences are very low, and dramatically increase (more than with SPALDI) while increasing the laser fluence, perhaps due to the increasing depth of penetration of the laser into the CHCA crystals or on cluster formation. The "reverse-notch" behavior in the curves of the molecular ion survival yields vs. laser fluences for CHCA might be caused by a superposition of ion energies formed in different penetration depths with the various fluences. We have also observed with CHCA an energy deposition dependence on the nature of rastering the target with the laser beam. The results in Fig. 2 are based on the integration of 50–200 laser shots while rastering the sample typically

Table 1
Critical energy and calculated lowest internal energy of BP ions generated by SPALDI with chemically modified and untreated Si nanoparticles, and by MALDI with CHCA. 70 ns was used as the reaction time in the calculation. The results represent the energy for a laser fluence that induced minimal, yet measurable fragmentation.

	Critical energy, E_0 (eV) [22]	Calculated lowest internal energy of BP ions (eV)				
		C10 modified Si	C6 modified Si	C3 modified Si	Untreated Si	CHCA
4-Cl BP	1.73	3.5	–	–	4.5	3.7
2-Me BP	1.64	3.4	–	–	4.2	3.6
4-Me BP	1.6	3.4	–	–	4.1	3.0
3-MeO BP	1.68	3.7	–	–	4.8	4.3
4-MeO BP	1.3	2.8	3.0	3.5	3.9	3.2

every 5–10 shots. Continuous shooting at a single point provided different results that seem to depend on the crystal morphology (“sweet spots”) and change upon “drilling” into the CHCA crystals.

The average internal energy of the BP ions formed by SPALDI and MALDI under various laser fluences in our experiments were determined by a previously reported method [19]. The calculated results are shown in Fig. 3 and Supplementary Data. The molecular survival yields were converted to experimental rate constants of unimolecular dissociations, k_{exp}, according to the equation:

$$k_{\mathrm{exp}} = -\left(\frac{1}{\tau}\right) \ \ln(\text{molecular survival yield})$$

where τ is defined as the reaction time in the accelerating region. The measurable reaction time was estimated as ~60–80 ns based on the source length and the voltages applied in the source region of our instrument. A value of 70 ns is used in the calculation of the internal energy for all the BP ions in our study. This value is comparable to the 100 ns used by Vertes and co-workers [19]. The reaction time in SPALDI as well as MALDI with organic matrices is believed to be similar since the BP ions are pre-charged and there is no proton transfer after the ions are desorbed from the silicon nanoparticles or the organic matrices. By making k_{exp} equal to k_{RRKM}, the internal energy of the BP ions can be determined from the curves of RRKM (Rice–Ramsperger–Kassel–Marcus) rate constants versus internal energy which were previously theoretically calculated [19]. As the internal energy calculation is based on the relative abundance of the molecular ions, the lowest internal energy, obtained at molecular survival yield = 100%, cannot be calculated and is therefore not included.

As the internal energy is inversely dependent on the molecular ion survival yield, the relationships between the energy curves for CHCA, and SPALDI with silylated and unsilylated particles, are similar to those on the survival curves. The lowest internal energy calculated for SPALDI and CHCA for all the BP ions is listed in Table 1. For SPALDI, the internal energies at the appearance threshold are the lowest internal energies that can be measured for the given reaction time as demonstrated in Fig. 3. The internal energy of BP ions desorbed from C10 modified Si nanoparticles is from 2.8 to 3.7 eV, where MALDI with CHCA generated BP ions with internal energy between 3.0 and 4.3 eV which is similar to the values of 3.3–4.1 eV for CHCA reported in the literature [19]. Table 1 shows that the internal energy of the BP ions generated by SPALDI with a C10 fluoroalkyl modifier (2.8 eV) is lower than that of ions desorbed in MALDI with CHCA near the threshold laser fluence (3.2 eV). Although 3-MeO BP and 4-MeO BP have a critical energy (E_0) difference of 0.4 eV, the difference in internal energy deposition of these two compounds with SPALDI, untreated silicon powder and CHCA is about ~1 eV. A similar phenomenon was observed in MALDI with organic matrices [19], indicating that the rate coefficient of the unimolecular decomposition is not determined solely by the critical energy and may be affected also by the structure of the compounds. The average internal energy calculated also clearly shows how the chain length of the chemical modifiers affects the internal energy deposition. The internal energy of the BP ions decreases with increasing chain length of the silylating modifiers from 3.5 eV with C3 to 3.0 eV with C6 to 2.8 eV with C10. With untreated silicon, the internal energy threshold (3.9 eV) is higher compared to that of the fluoroalkyl-modified powder (2.8–3.5 eV) or MALDI with CHCA (3.2 eV). Compared to the critical energy of BP ions reported in the literature [22], silicon nanoparticles modified with C10 fluoroalkyl chains can deposit internal energy as low as 1.5–2 eV to BP ions upon LDI, while CHCA generally deposits more than 2 eV internal energy to BP ions as they are desorbed and ionized. Therefore SPALDI with C10 fluoroalkyl modifier is a slightly “softer” ionization method than MALDI with CHCA. The untreated silicon nanoparticles deposit more than 2.5 eV internal energy to the BP ions upon LDI, generating more fragmentation compared to SPALDI and MALDI with CHCA.

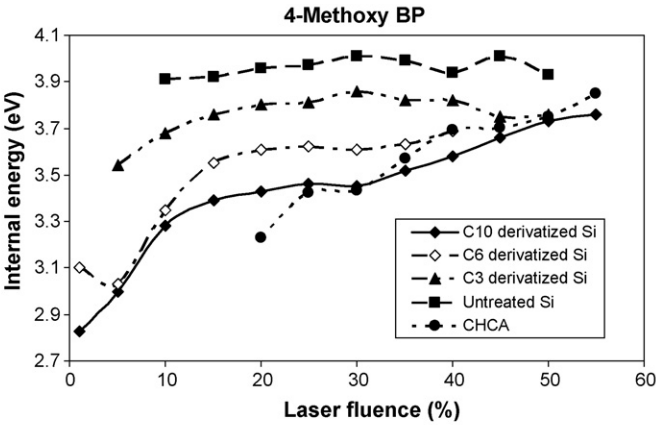

Fig. 3. Internal energy deposition calculated for 4 methoxy BP. SPALDI with C10 modified particles (♦), untreated silicon powder (■), CHCA (●), SPALDI with C6 derivatized particles (◇), and SPALDI with C3 derivatized particles (▲). The laser fluence is shown in percentage of the total nitrogen laser fluence. Typical variance of the reported internal energy deposition is 2–10%.

4. Conclusions

The data presented here indicate that for the BP model compounds, SPALDI with C10 silylated silicon nanoparticles induces survival yields of the molecular ions similar or higher (at the threshold fluence range) than the conventional CHCA matrix. The survival yields shown for SPALDI are also comparable to those measured for silicon nanowires [13], although, interestingly, the SPALDI-induced internal energy always increases with the laser fluence, whereas with silicon nanowires it is reported to be slightly decreasing with the laser fluence.

DIOS, which is based on chemically modified nanopores on a silicon substrate, has previously been reported to have much lower survival yields and much higher laser fluence thresholds [21]. Similarly low survival yields have been reported for DIOS from various chemical modifiers, including the semi-fluoroalkyl chain also used in SPALDI experiments.

The nanostructure of silicon (particles or nanowires) is therefore believed to induce effective local heating, resulting in vaporization of the analytes at lower laser fluences [13] that may result in more uniform energy deposition, inducing "softer" LDI. The large surface area of nanostructured silicon may also contribute to the lower laser fluence required to induce LDI [25]. It is noted that SPALDI with C10 fluoroalkyl-modifier induces sufficient signals even at a minimal laser fluence (1–5%), which makes the operation of SPALDI at those fluences practical.

The BP model compounds are precharged ions, thus, similarly to previous studies with BP ions [13,19–21], it is assumed that this study represents internal energies originated by heat transfer only. This is usually not the case with standard chemical matrices in MALDI, where proton transfer may also take place during the LDI process and significantly affect the internal energy of the formed ions [15]. It is believed, however, that with SPALDI, which is a highly selective method, the effective mechanism is LDI of precharged ions [12] and charge transfer is less likely to occur during LDI.

The high survival yields of molecular ions in SPALDI experiments at low laser fluences, demonstrated here, reveal a potential for improved analytical performance in the analysis of labile compounds that should be further explored with this new approach.

Acknowledgments

The authors are grateful to Xiujuan Wen, for her contribution during the early stages of this work. The financial support of NSF-CHE grant No. 0416338 is appreciated.

Appendix A. Supplementary data

Supplementary data associated with this article can be found, in the online version, at doi:10.1016/j.ijms.2009.03.013.

References

[1] M. Karas, F. Hillenkamp, Laser desorption ionization of proteins with molecular masses exceeding 10000 Daltons, Analytical Chemistry 60 (20) (1988) 2299–2301.

[2] J. Wei, J.M. Buriak, G. Siuzdak, Desorption–ionization mass spectrometry on porous silicon, Nature 399 (6733) (1999) 243–246.

[3] Z.X. Shen, J.J. Thomas, C. Averbuj, K.M. Broo, M. Engelhard, J.E. Crowell, M.G. Finn, G. Siuzdak, Porous silicon as a versatile platform for laser desorption/ionization mass spectrometry, Analytical Chemistry 73 (3) (2001) 612–619.

[4] J.J. Thomas, Z.X. Shen, R. Blackledge, G. Siuzdak, Desorption–ionization on silicon mass spectrometry: an application in forensics, Analytica Chimica Acta 442 (2) (2001) 183–190.

[5] W.G. Lewis, Z.X. Shen, M.G. Finn, G. Siuzdak, Desorption/ionization on silicon (DIOS) mass spectrometry: background and applications, International Journal of Mass Spectrometry 226 (1) (2003) 107–116.

[6] S.A. Trauger, E.P. Go, Z.X. Shen, J.V. Apon, B.J. Compton, E.S.P. Bouvier, M.G. Finn, G. Siuzdak, High sensitivity and analyte capture with desorption/ionization mass spectrometry on silylated porous silicon, Analytical Chemistry 76 (15) (2004) 4484–4489.

[7] T. Kinumi, T. Saisu, M. Takayama, H. Niwa, Matrix-assisted laser desorption/ionization time-of-flight mass spectrometry using an inorganic particle matrix for small molecule analysis, Journal of Mass Spectrometry 35 (3) (2000) 417–422.

[8] S.Y. Xu, Y.F. Li, H.F. Zou, J.S. Qiu, Z. Guo, B.C. Guo, Carbon nanotubes as assisted matrix for laser desorption/ionization time-of-flight mass spectrometry, Analytical Chemistry 75 (22) (2003) 6191–6195.

[9] C.S. Pan, S.Y. Xu, L.G. Hu, X.Y. Su, J.J. Ou, H.F. Zou, Z. Guo, Y. Zhang, B.C. Guo, Using oxidized carbon nanotubes as matrix for analysis of small molecules by MALDI-TOF MS, Journal of the American Society for Mass Spectrometry 16 (6) (2005) 883–892.

[10] E.P. Go, J.V. Apon, G. Luo, A. Saghatelian, R.H. Daniels, V. Sahi, R. Dubrow, B.F. Cravatt, A. Vertes, G. Siuzdak, Desorption/ionization on silicon nanowires, Analytical Chemistry 77 (6) (2005) 1641–1646.

[11] G.M. Credo, E.S.P. Bouvier, Small molecule TOF MS detection using nanoscale particles compared to analyte detection using DIOS substrates, in: Proceedings of the 52nd ASMS Conference on Mass Spectrometry and Allied Topics, Nashvillie, TN, USA, May 23–27, 2004.

[12] X.J. Wen, S. Dagan, V.H. Wysocki, Small-molecule analysis with silicon-nanoparticle-assisted laser desorption/ionization mass spectrometry, Analytical Chemistry 79 (2) (2007) 434–444.

[13] G.H. Luo, Y. Chen, H. Daniels, R. Dubrow, A. Vertes, Internal energy transfer in laser desorption/ionization from silicon nanowires, Journal of Physical Chemistry B 110 (27) (2006) 13381–13386.

[14] Q. Zhan, S.J. Wright, R. Zenobi, Laser desorption substrate effects, Journal of the American Society for Mass Spectrometry 8 (5) (1997) 525–531.

[15] E. Stevenson, K. Breuker, R. Zenobi, Internal energies of analyte ions generated from different matrix-assisted laser desorption/ionization matrices, Journal of Mass Spectrometry 35 (8) (2000) 1035–1041.

[16] R. Dale, R. Knochenmuss, R. Zenobi, Two-phase matrix-assisted laser desorption/ionization: matrix selection and sample pretreatment for complex anionic analytes, Rapid Communications in Mass Spectrometry 11 (1) (1997) 136–142.

[17] V. Gabelica, E. Schulz, M. Karas, Internal energy build-up in matrix-assisted laser desorption/ionization, Journal of Mass Spectrometry 39 (6) (2004) 579–593.

[18] E. Schulz, M. Karas, F. Rosu, V. Gabelica, Influence of the matrix on analyte fragmentation in atmospheric pressure MALDI, Journal of the American Society for Mass Spectrometry 17 (7) (2006) 1005–1013.

[19] G.H. Luo, I. Marginean, A. Vertes, Internal energy of ions generated by matrix-assisted laser desorption/ionization, Analytical Chemistry 74 (24) (2002) 6185–6190.

[20] A. Vertes, G.H. Luo, L. Ye, Y. Chen, I. Marginean, Laser pulse length dependence of internal energy transfer in UV-MALDI-MS, Applied Physics A: Materials Science & Processing 79 (4–6) (2004) 823–825.

[21] G.H. Luo, Y. Chen, G. Siuzdak, A. Vertes, Surface modification and laser pulse length effects on internal energy transfer in DIOS, Journal of Physical Chemistry B 109 (51) (2005) 24450–24456.

[22] C. Collette, L. Drahos, E. De Pauw, K. Vekey, Comparison of the internal energy distributions of ions produced by different electrospray sources, Rapid Communications in Mass Spectrometry 12 (22) (1998) 1673–1678.

[23] P.C. Rusu, G. Brocks, Surface dipoles and work functions of alkylthiolates and fluorinated alkylthiolates on Au(1 1 1), Journal of Physical Chemistry B 110 (45) (2006) 22628–22634.

[24] T.R. Northen, O. Yanes, M.T. Northen, D. Marrinucci, W. Uritboonthai, J. Apon, S.L. Golledge, A. Nordstrom, G. Siuzdak, Clathrate nanostructures for mass spectrometry, Nature 449 (7165) (2007) 1033–1043.

[25] T.R. Northen, H.K. Woo, M.T. Northen, A. Nordstrom, W. Uritboonthail, K.L. Turner, G. Siuzdak, High surface area of porous silicon drives desorption of intact molecules, Journal of the American Society for Mass Spectrometry 18 (11) (2007) 1945–1949.